

Particle-Based Simulation of Shock-Induced Deformation of Elastic Bodies

Y. Sakamura, T. Sugimoto, and K. Nakayama

1 Introduction

Shock-induced deformations of solid bodies are of practical interest to those who are concerned with explosive processing of materials, demolition of buildings, precautions against accidental explosions, *etc.* In order to simulate the shock-induced deformations of solid bodies, a large number of numerical codes based on continuum mechanics, which are called hydrocodes, have been developed so far [1, 2]. When the amount of deformation is relatively small, Lagrangian hydrocodes have been used to simulate the dynamic response of shock-loaded materials. When the deformation is large, Eulerian hydrocodes have been utilized instead. This is because the computational grids distorted along with the deformation of materials in the Lagrangian approach make the simulations either inaccurate or unstable, while the Eulerian approach where grids are fixed in space can handle such large deformations of materials. On the contrary, material interfaces that are precisely defined in the Lagrangian approach are not traced exactly in the Eulerian one.

To resolve the deficiencies of the grid-based methods such as mentioned above, alternative methods named particle methods have been proposed [3]. In the particle methods, the governing equations are discretized using moving particles and their interactions. Driven by interaction forces determined from the discretized form of the governing equations, each particle moves in Lagrangian coordinates. The advantages of the particle methods are that there is no need to trace the material interfaces and that the calculation will continue to run regardless of the amount of deformation. In the present work, we have developed a particle-based simulation code for shock-induced deformation problems based on the Moving Particle Semi-implicit (MPS) method, which was originally developed for incompressible fluid flow simulations [4, 5], and applied it to large deformation of a rubber rod caused by a shock impingement to examine its feasibility.

Y. Sakamura · T. Sugimoto · K. Nakayama

Department of Mechanical Systems Engineering, Toyama Prefectural University
5180 Kurokawa, Imizu, Toyama 939-0398, Japan

2 Numerical Method

2.1 Governing Equations

In developing the governing equations for the dynamics of an elastic body (rubber), we assume that: (a) the body is an isotropic elastic medium and the change in its internal energy is negligibly small, and (b) friction and gravity forces acting on the body are negligibly small. Under these assumptions, the governing equations are given as

$$\frac{Dr_\alpha}{Dt} = v_\alpha, \quad \rho \frac{Dv_\alpha}{Dt} = \frac{\partial}{\partial x_\beta} (\lambda \varepsilon_{\gamma\gamma} \delta_{\alpha\beta} + 2\mu \varepsilon_{\alpha\beta}) \quad (1)$$

where r_α : position vector, t : time, D/Dt : the substantial derivative, v_α : velocity, ρ : density, x_α : the Cartesian coordinates, λ , μ : Lamé's constants, $\delta_{\alpha\beta}$: Kronecker's delta, $\varepsilon_{\alpha\beta}$: strain tensor, and the subscripts α, β, γ represent standard tensorial notation.

2.2 Particle Interaction Models

In the MPS method, the elastic material is expressed by moving particles, and the differential operators in the governing equations are discretized by using several particle interaction models. The gradient of arbitrary scalar quantity ϕ can be approximated by the average of gradient between particle i and neighboring particle j as

$$\langle \nabla \phi \rangle_i = \frac{d}{n^0} \sum_{j \neq i} \frac{\phi_j - \phi_i}{|\mathbf{r}_j - \mathbf{r}_i|} \frac{\mathbf{r}_j - \mathbf{r}_i}{|\mathbf{r}_j - \mathbf{r}_i|} w(|\mathbf{r}_j - \mathbf{r}_i|) \quad (2)$$

where d is the number of space dimension (2 for two-dimensional and 3 for three-dimensional fields), n^0 is the initial number density of particles, and $w(r)$ is the weight of interaction between two particles that are a distance of $r = |\mathbf{r}_j - \mathbf{r}_i|$ apart and given as

$$w(r) = \begin{cases} r_e/r - 1 & \text{if } 0 < r < r_e \\ 0 & \text{if } r_e \leq r \end{cases}$$

Here r_e is the radius of the interaction area and set to be $2.1l_0$ (l_0 : initial distance between the particles). Similarly, the divergence of arbitrary vector quantity \mathbf{u} can be given as the average of those between particle i and neighboring particle j :

$$\langle \nabla \cdot \mathbf{u} \rangle_i = \frac{d}{n^0} \sum_{j \neq i} \frac{\mathbf{u}_j - \mathbf{u}_i}{|\mathbf{r}_j - \mathbf{r}_i|} \cdot \frac{\mathbf{r}_j - \mathbf{r}_i}{|\mathbf{r}_j - \mathbf{r}_i|} w(|\mathbf{r}_j - \mathbf{r}_i|) \quad (3)$$

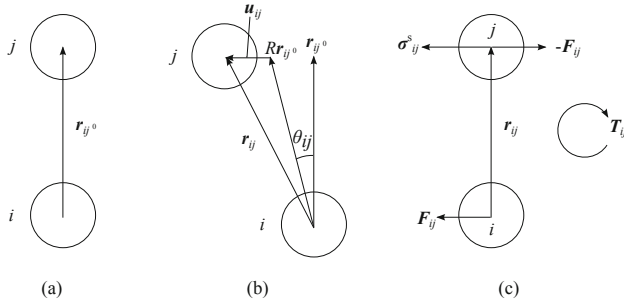


Fig. 1 (a) Initial position vector of particle j relative to particles i , (b) displacement vector of particle j relative to particle i and (c) torque induced by the shear stress between particles i and j

2.3 Method of Solution

In the MPS method for two-dimensional problems such as considered in the present work, the motion of each particle can be expressed by a two-dimensional position vector \mathbf{r} and its time derivative (velocity \mathbf{v}), and a rotational angle around the center of the particle θ and its time derivative (angular velocity ω), all of which are functions of time t .

When the position vector of particle j relative to particle i is given by $\mathbf{r}_{ij} = \mathbf{r}_j - \mathbf{r}_i$, the relative displacement between particles i and j , \mathbf{u}_{ij} is expressed as $\mathbf{u}_{ij} = \mathbf{r}_{ij} - R(\theta_{ij})\mathbf{r}_{ij}^0$, where \mathbf{r}_{ij}^0 is the initial relative position vector and $R(\theta_{ij})$ is the matrix representing a rotation through an angle $\theta_{ij} = (\theta_i + \theta_j)/2$ about the center of the particle i (see Fig. 1),

$$R(\theta_{ij}) = \begin{bmatrix} \cos \theta_{ij} & -\sin \theta_{ij} \\ \sin \theta_{ij} & \cos \theta_{ij} \end{bmatrix} \quad (4)$$

The normal stress σ_{ij}^n (stress component parallel to \mathbf{r}_{ij}) and the shear stress σ_{ij}^s (stress component perpendicular to \mathbf{r}_{ij}) are then obtained from the following relations: $\sigma_{ij}^n = 2\mu \varepsilon_{ij}^n = 2\mu \mathbf{u}_{ij}^n / |\mathbf{r}_{ij}^0|$ and $\sigma_{ij}^s = 2\mu \varepsilon_{ij}^s = 2\mu \mathbf{u}_{ij}^s / |\mathbf{r}_{ij}^0|$, where \mathbf{u}_{ij}^n and \mathbf{u}_{ij}^s are the normal and the shear components, respectively, of the relative displacement \mathbf{u}_{ij} . Also, the pressure at the position of particle i can be defined as $p_i = -\lambda (\varepsilon_{\gamma\gamma})_i$, where the trace of the strain tensor $(\varepsilon_{\gamma\gamma})_i$ is calculated using the divergence model (Eq. 3). The contributions from these stress components to the acceleration of particle i is separately computed as follows.

$$\left(\frac{D\mathbf{v}}{Dt}\right)_i^{n \text{ (or } s)} = \frac{d}{\rho n^0} \sum_{j \neq i} \frac{2\sigma_{ij}^{n \text{ (or } s)}}{|\mathbf{r}_{ij}^0|} w(|\mathbf{r}_{ij}^0|), \quad \left(\frac{D\mathbf{v}}{Dt}\right)_i^p = -\frac{d}{\rho n^0} \sum_{j \neq i} \frac{2p_{ij}\mathbf{r}_{ij}}{|\mathbf{r}_{ij}^0||\mathbf{r}_{ij}|} w(|\mathbf{r}_{ij}^0|) \quad (5)$$

where $p_{ij} = (p_i + p_j)/2$. The acceleration of particle i is finally obtained from the summation of these contributions:

$$\left(\frac{D\mathbf{v}}{Dt}\right)_i = \left(\frac{D\mathbf{v}}{Dt}\right)_i^n + \left(\frac{D\mathbf{v}}{Dt}\right)_i^s + \left(\frac{D\mathbf{v}}{Dt}\right)_i^p \tag{6}$$

In the MPS method for elastic problems, a torque $-\mathbf{T}_{ij}/2$ is applied to particles i and j in order to conserve the angular momentum of the system, where T_{ij} is the torque induced by the shear force \mathbf{F}_{ij} between the two particles with the same mass m (see Fig. 1 (c)) and given by

$$\mathbf{T}_{ij} = -\mathbf{r}_{ij} \times \mathbf{F}_{ij}, \quad \mathbf{F}_{ij} = m \left(\frac{D\mathbf{v}}{Dt}\right)_{ij}^s = \frac{m}{\rho} \frac{2d}{n^0} \frac{\sigma_{ij}^s}{|\mathbf{r}_{ij}^0|} w(|\mathbf{r}_{ij}^0|) \tag{7}$$

The following equation of rotational motion is then solved for two-dimensional problems: $I_i(D\omega/Dt)_i = -1/2 \sum_{j \neq i} T_{ij}$, where I_i is the moment of inertia of particle i about its center of mass.

The velocity, position, angular velocity, and rotational angle of each particle are finally updated as follows.

$$\mathbf{v}_i^{k+1} = \mathbf{v}_i^k + \Delta t \left(\frac{D\mathbf{v}}{Dt}\right)_i^k, \quad \mathbf{r}_i^{k+1} = \mathbf{r}_i^k + \Delta t \mathbf{v}_i^{k+1} \tag{8}$$

$$\omega_i^{k+1} = \omega_i^k + \Delta t \left(\frac{D\omega}{Dt}\right)_i^k, \quad \theta_i^{k+1} = \theta_i^k + \Delta t \omega_i^{k+1} \tag{9}$$

where the superscript k is the time level and Δt is the time interval during the numerical time integration.

2.4 Numerical Conditions and the Treatment of the Motion of a Rigid Body

Figure 2 schematically illustrates the problem to be solved, which is similar to one of those in [6]. A normal shock wave propagates from left to right at a constant velocity and at time $t = 0$ it collides head-on with a rigid plate (60 mm \times 6 mm), which is supported by a rubber rod (40 mm \times 100 mm). The step-like force resulting from the head-on collision of the shock wave with the rigid plate is applied on the left-hand side of the rubber rod and the rubber rod then starts deforming. The rubber rod is fixed on a rigid wall as shown in Fig. 2 and its expansion in the direction normal to the page is also restricted by other, two rigid walls (not shown), so that it deforms two-dimensionally under the biaxial stress condition. The time step size Δt during the numerical integration was set to be 10 ns, which was determined from preliminary simulations with different step sizes.

In the present work, the motion of the rigid plate attached to the rubber rod was also simulated in a similar particle-based fashion [7]. When a rigid body is composed of N particles with the same mass m , the center of gravity \mathbf{r}_g and moment of inertia I of the rigid body are represented by $\mathbf{r}_g = \sum_{i=1}^N \mathbf{r}_i / N$ and $I = m \sum_{i=1}^N |\mathbf{r}_i - \mathbf{r}_g|^2$, respectively. In each time step, the motion of each particle is calculated using

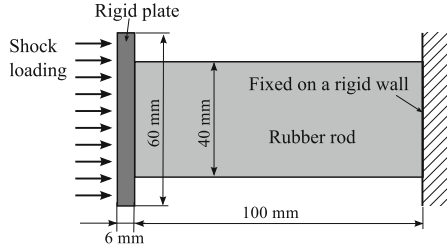


Fig. 2 Schematic description of the problem to be solved

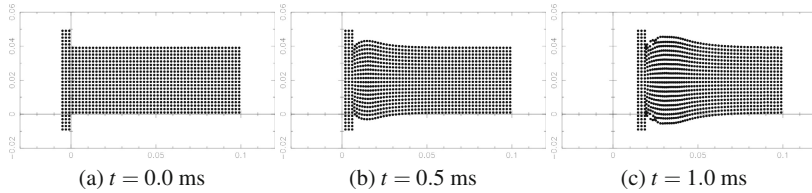


Fig. 3 Nonphysical results obtained from the simulation with $F = 55.9$ kN

the same procedure with that of the rubber particles at first. The translational and angular velocities of the rigid body are then evaluated as $\mathbf{V} = \sum_{i=1}^N \mathbf{v}_i / N$ and $\mathbf{R} = m \sum_{i=1}^N \mathbf{v}_i \times (\mathbf{r}_i - \mathbf{r}_g) / I$, respectively. The velocity of each rigid particle is finally replaced by $\mathbf{v}_i = \mathbf{V} + (\mathbf{r}_i - \mathbf{r}_g) \times \mathbf{R}$ to keep the distances between all pairs of them constant.

3 Results

Representative results from the present simulations are shown in Figs. 3 and 4, where the location of each particle is designated by a dot and a set of successive results saved 1.0 ms apart are presented. In the case shown here, the two-dimensional rubber rod is represented by 20×50 particles ($l_0 = 2$ mm), and the rigid plate was represented by 30×3 particles with the same density as the rubber. The particle number of the rubber rod was determined from preliminary simulations with different particle numbers. The Young’s modulus (E), Poisson’s ratio (ν) and density (ρ) of the rubber were set to be the same as those in the experiment by Mazor et al. [6]; $E = 2.8$ MPa, $\nu = 0.495$, $\rho = 1.01$ kg/m³. When, however, the force equivalent to that in the experiment ($F = 55.9$ kN) was applied, the numerical simulation exhibited an unphysical behavior and finally blew up as shown in Fig. 3. The force applied to the rubber rod in the case shown in Fig. 4 was so reduced 11.2 kN that physically reasonable results could be obtained. For comparison, shadowgraphs obtained from the shock tube experiment [6] are shown in Fig. 5. The rubber compression in the horizontal direction and its expansion in the vertical direction are clearly seen in these figures. Although the applied force is different from that in

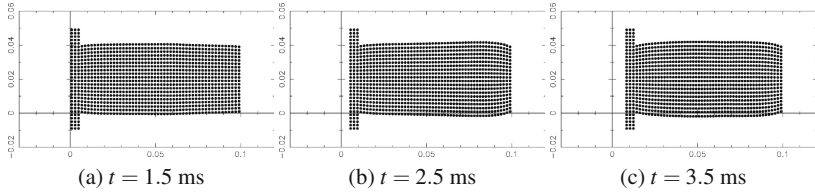


Fig. 4 Results obtained from the simulation with $F = 11.2$ kN

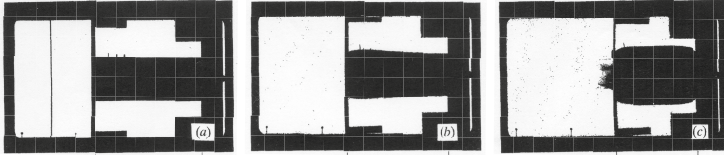


Fig. 5 Shadowgraphs obtained from the shock tube experiment [6]. The time elapsed between successive frames is 1.2 ms.

the experiment, the simulated response of the shock-loaded rubber rod qualitatively agrees with that observed in the experiments.

4 Conclusion

A particle-based simulation code has been developed for shock-induced deformation problems and applied to the large deformation of a rubber rod caused by the head-on collision of a shock wave. Typical features of the response of the shock-loaded rubber rod observed in shock tube experiments are successfully reproduced by using the present code. Future work will be directed to improve its robustness under high loading conditions and to apply it to fluid-structure interaction problems.

Acknowledgment. The authors would like to thank Yu Hamazaki for his help in fixing the bugs in our code. This work was supported by JSPS KAKENHI Grant Number 22510181.

References

1. Anderson Jr., C.E.: *Int. J. Impact Eng.* 5 (1987)
2. Benson, D.J.: *Comp. Methods in Applied Mech. Eng.* 99 (1992)
3. Li, S., Liu, W.: *Applied Mech. Rev.* 55 (2002)
4. Koshizuka, S., Oka, Y.: *Nucl. Sci. Eng.* 123 (1996)
5. Koshizuka, S., Chikazawa, Y., Oka, Y.: Particle method for fluid and solid dynamics. In: Bathe, K.J. (ed.) *Proc. 1st MIT Conf. on Comp. Fluid & Solid Mech.*, pp. 1269–1271. Elsevier (2001)
6. Mazor, G., Igra, O., Ben-Dor, G., Mond, M., Reichenbach, H.: *Phil. Trans. R. Soc. Lond. A* 338 (1992)
7. Koshizuka, S., Nobe, A., Oka, Y.: *Int. J. for Num. Method in Fluids* 26 (1998)